RESEARCH PAPER

Chlorogenic acid, isolated from the plant, Eupatorium glandulosum promotes the expression of TNF-α, IL-18 and MMP-9 during early wound healing: In vitro, in silico and dynamic simulation and In vivo Analysis.

Shalini R[1*], Moola Joghee Nanjan Chandrasekar[2], Nanjan Moola Joghee[3]

[1,2]school Of Life Sciences, Jss Academy Of Higher Education & Research (Ooty Campus), Longwood, Mysuru Road, Ooty, The Nilgiris-643001, Tamilnadu, India;

[3]masi Consultants, Vijayanagar Palace Road, Ooty, Nilgiris-643001

[*]**Corresponding Author:** Dr. R. Shalini

School Of Life Sciences, Jss Academy Of Higher Education & Research (Ooty Campus), Longwood, Mysuru Road, Ooty, The Nilgiris-643001, Tamilnadu , India.

E-Mail: shalinir@Jssuni.Edu.In

Received: 12th Mar, 2026 | **Revised:** 24th Mar, 2026 | **Accepted:** 14th Apr, 2026 | **Available Online:** 30th Apr, 2026

ABSTRACT

Background:

The plant, Eupatorium glandulosum H. B & K, has been traditionally used to treat wounds and cuts in Nilgiris District, India.

Aim of the study:

The purpose of this study was to investigate the wound healing potential of plant extract and isolated compound, Chlorogenic acid from the plant, Eupatorium glandulosum, confirm its structure by spectral and other studies.

Materials and Methods:

The plant methanolic extract was evaluated for its viability and migration using mouse fibroblast NIH3T3 cell lines. Chlorogenic acid was isolated from the plant methanolic extract and examined for its viability, migration, qPCR analysis, in addition to in silico, MM/GBSA, molecular simulation and in vivo studies.

Results:

The plant methanolic extract at the concentration of 31.25, 62.5, 125 µg/ml shows 100% of wound closure at 48h. The Chlorogenic acid was isolated from methanolic extract and at the concentration of 800, 1600, 3200µM shows 99% wound closure at 24h. The binding energy of the compound with the wound healing markers, TNF-α, IL-12, IL-18, GM-CSF, MMP-2 and MMP-9 is -7.3, -6, -8.1, -6.8, -7 and -9.4 kcal/mole, respectively. The compound thus shows the lowest binding energy with MMP-9 and hence Chlorogenic acid-MMP-9 complex was subjected to MM/GBSA and molecular simulation studies. The binding free energy of the Chlorogenic acid-MMP-9 complex is 46.45992076 kcal/mol which shows strong binding of the ligand with the protein, MMP-9. The RMSF values of MMP-9 protein are stable near 70-85 and 120-140 residue index that is in α helix and β sheet, respectively. GLN227 and Asp235 amino acids are responsible for the strong binding. Water bridges also play a major role in binding. Gene expression analysis shows the release of IL-18, TNF-α and MMP-9 at early stages of healing and the complete wound closure at 28th day. In vivo studies reveal that the compound at 2% concentration shows 94.18% wound contraction comparable to nitrofurazone. Histological studies reveal by significant collagen content, inflammatory cells and angiogenesis.

Conclusion

Chlorogenic acid is, therefore, a possible drug/lead. Further work is in progress.

Keywords:

Eupatorium glandulosum, wound healing, Chlorogenic acid, MM/GBSA, molecular dynamics, molecular docking

Abbreviation

ADME: Absorption, Distribution, Metabolism and Excretion, GM-CSF: Granulocyte macrophage colony stimulating factor, IL-18: Interleukin-18, MMP-9: Matrix metalloproteinase 9, MM/GBSA: Molecular

mechanics-generalized Born surface area, qPCR: Quantitative polymerase chain reaction, SRB: Sulforhodamide B, Tnf-α: Tumour necrosis factor alpha

How to cite this article: Shalini R, Moola Joghee Nanjan Chandrasekar, Nanjan Moola Joghee, Chlorogenic Acid, Isolated From The Plant, Eupatorium Glandulosum Promotes The Expression Of TNF-A, IL-18 And MMP-9 During Early Wound Healing: In Vitro, In Silico And Dynamic Simulation And In Vivo Analysis. Int J Drug Deliv Technol. 2026;16(5): 1471-1487. DOI: 10.25258/ijddt.16.5.137

INTRODUCTION

Wound healing is a highly complicated mechanism in which chemokine, cytokines, growth factors and various cells that include neutrophil, leukocytes, macrophages, fibroblasts and keratinocytes are coordinates to restore the damaged tissue [1]. Wound healing remains a challenging clinical problem due to the prolongation of proinflammatory cytokines and high level of proteolytic enzyme. The molecular mechanism of wound healing has been investigated for decades but an effective therapy is still at infancy. Natural product therapies are, therefore, widely utilized today because of its affordability, reliability and safety though not very efficacious [2].

An effective therapy should be based on the understanding of the molecular pathways, namely at which phase wound healing is halted and leads to complications. The molecular mechanism of some of the natural products have been explored. However, the targets of several natural products have not been thoroughly explored due to their unclear mechanism of action [3]. Quercetin 3-O-glucoside from the traditional wound healing plant, *Sambucus ebulus* L [4], Lupane triterpenoid from the Ghanaian traditional wound healing plant, *Paullinia pinnata* [5], 2-(3,4-dihydroxy-phenyl)-5,7-dihydroxy-chromen-4-one and 1, 2-tetradecanediol, 1-(hydrogen sulfate) from the Indian traditional wound healing plant, *Pedilanthus tithymaloides* [6], protocatechuic acid from Indian traditional wound healing plant, *Trianthema portulcastrum* have shown significant wound healing activity [7]. The wound healing target of Quercetin 3-O-glucoside, 2-(3,4-dihydroxy-phenyl)-5,7-dihydroxy-chromen-4-one and 1, 2-tetradecanediol, 1-(hydrogen sulfate), protocatechuic acid are yet to be explored.

The non-healing wounds are characterised by high levels of proinflammatory cytokines and proteolytic enzymes. Neutrophils and macrophages are major producers of proinflammatory cytokines. These include IL-1α, IL-1β, IL-6, IL-18, and TNF-α that are upregulated during the inflammatory phase of wound healing. These cytokines activate immune cells and prevent infection. They also play a major role in remodelling of the damaged tissues by regulating fibroblasts and epithelial cells in healing [8].

The plant, *Eupatorium glandulosum,* has been traditionally used to treat wounds and cuts by the Toda, Irula and Badaga, tribal community of the Nilgiris district, India [9]. In recent years pharmacologically active compounds from traditional plants have received greater insight into the structure-activity relationships as they are a source of novel pharmacophores in drug discovery process [10]. In the present study, Chlorogenic acid was isolated from the plant, *Eupatorium glandulosum*, by bioguided fractionation, the bioactive compound docked with different wound healing markers, namely TNF-α, IL-1, IL-12, IL-18, GM-CSF, MMP-2 and MMP-9 and evaluated by qPCR and *in vivo* for its wound healing potential.

MATERIALS AND METHODS

Plant Collection

The aerial parts of the plant was collected during October 2020 from Udhagamandalam, Nilgiris district, India, and identified by Prof R. Ravi from Government Arts College, Udhagamandalam.

Extraction and Isolation

The plant fresh leaves were extracted with methanol by maceration. Methanol was removed under reduced pressure. The dry extract was fractionated by solvents such as petroleum ether, chloroform and ethyl acetate [11]. The ethyl acetate residue was subjected to column chromatography by increasing the concentration of ethanol in benzene to obtain Chlorogenic acid.

Spectral Studies

The compound was identified using $_{1}H$ and $_{13}C$ NMR, FTIR and LCMS/MS. The spectrum of the isolated compound was confirmed with literature data.

In Vitro Studies

In Vitro Cell Viability Assay of Chlorogenic Acid by SRB

Viability of Chlorogenic acid treated Human keratinocyte (HaCaT cell line) was evaluated using SRB assay [12]. The cells ($1*10^4$cells/well) were seeded in 200µL of DMEM media and incubated at 37^0 C with 5% CO_2 for 36 h. After the cells reached 60-70% confluency, they were exposed to different concentrations of Chlorogenic acid ranging from 100µM to 3200µM and incubated at 37^0C with 5% CO_2 for 24 h. After 24h, the cells were fixed with the help of 50µl of 50% trichloroacetic acid and incubated for 60 min at 4^0C. The plate was washed with tap water and dried to remove trichloroacetic acid and excessive water. Sulforhodamide B (100 µl) dye was added to the well plate to stain the cellular protein. Acetic acid (1%) was added to each well to remove the unbound dye. The dye was dissolved by adding 100 µl of 10 mM tris base solution and the absorbance was determined at 510 nm using the microplate reader. DMSO and Cisplatin (100µM) were used as the control group and standard group, respectively. The cell viability (%) was determined using the formula, Cell viability (%) = Absorbance of the test sample/absorbance of the control*100

Scratch Wound Healing Assay

The migratory potential of Chlorogenic acid was assessed by Scratch wound healing assay [13-14]. HaCaT cells were seeded into each well to reach a final concentration of $0.5*10^6$ cells/well. A 12 well plate was incubated for 24 h at 37^0 C. Sufficient incubation time was allowed for the cells to attach to the substrate and achieve 80% confluent monolayer. A mechanical wound was created by scraping the monolayer with an approximate width of 0.7mm using 10µl sterile pipette tip. Chlorogenic acid was serially diluted with DMSO to obtain 800, 1600 and 3200 µM concentrations. DMSO and itraconazole (5µg/ml) were used as vehicle control and standard, respectively. After treating with Chlorogenic acid, the plates were incubated for 12 h at 37^0 C with 5% CO_2. The keratinocyte migration was evaluated every 6 h till 24h. The migration of keratinocytes to close the scratch wound was photographed and quantified by imageJ. The scratch wound assay was carried out in triplicates. The difference between initial wound area and final wound area was calculated using the formula,

% wound closure= wound area at initial time-wound at n time/ wound area at initial time*100

In Silico Docking

The *in silico* studies were performed by using drug design softwares PyRx, discovery studio and Schrodinger suite 2021-4.

Pyrex language was downloaded from www.pyrex.com. Discovery Studio visualizer 4.1 was downloaded from www.accelerys.com [15].

Preparation of Target Molecule

The 3D structure of the human TNF-α (PDB ID-2AZ5), IL-12 (PDB ID-6WDP), IL-18 (PDB ID-4R6U), GM-CSF (PDB ID-5D71), MMP-2 (PDB ID-1HOV) and MMP-9 (PDB-4H1Q) were collected from the Protein data bank (PDB: http:// www. rcsb. org/ pdb). These wound healing targets were prepared using PyRx embedded with Autodock and Discovery Studio Visualizer to perform docking. The target proteins were cleaned by removing the co-crystals, heteroatoms and water molecules before analysis. Hydrogen atoms were also added to the target proteins. Energy minimization was employed through Swiss-PDB Viewer force field. The precision of the target protein structures was validated by Ramachandran plot. The PDB files were converted to PDBQT files for further analysis.

Preparation of Ligand

The chemical structure of Chlorogenic acid was drawn using Marvin sketch tools. The structure was optimized and converted to PDBQT module of PyRx version 0.9 for further analysis.

Molecular Docking

The interaction of Chlorogenic acid with wound healing targets was analysed by molecular docking using PyRx version 0.9. The ligand was screened against various wound healing targets. Docking was carried out by using Autodock vina programme. The ligand-receptor complex was further evaluated using MM/GBSA and simulation study.

Pharmacokinetic, Physicochemical Properties and Toxicity Prediction Analysis

The Swiss ADME online web tool (http://www. swiss adme. ch/) and PreADMET (https://preadmet.webservice.bmdrc.org/toxicity/) server were used to screen the pharmacokinetic & physicochemical and toxicity features of Chlorogenic acid, respectively.

Mm/Gbsa

Molecular docking was further evaluated using MM/GBSA to calculate the binding free energy of chlorogenic acid-MMP-9 complex and post docking energy minimization study. The free

energy was calculated using MM/GBSA of Schrödinger 2021-4 suite. The energy minimization was done using OPLS4 force field [16].

Molecular Dynamics Simulation

The stability of binding between the bioactive compound, Chlorogenic acid and the wound healing target, MMP-9, was assessed by molecular dynamic simulation studies utilizing desmond module of Schrodinger suit 2021-4. The complex, chlorogenic acid-MMP-9, was solvated by adding water molecule and ionised using Na^+, Cl^- ions. The 100ns simulation study was performed with 2 fs time under isothermal-isobaric ensemble at a temperature of 300K and 1bar pressure. The neutralization of the solvated system was performed using 0.15M Na^+ Cl^- counter ions. The force field was minimised using OPLS3e. The long range electric forces between the atoms were calculated using smooth particle mesh Ewald method with 1e-09 tolerance. The short range Van der Waals and Coulomb interactions were calculated at cut-off radius of 9.0 A. A constant temperature of 300K and pressure of 1 bar were maintained using an ensemble of Nose-Hoover thermostat and barostat, respectively. Multiple time step RESPA integration was utilised in the dynamic study to evaluate bonded, short-range non-bonded and long range electrostatic forces with 2, 2 and 6 fs, respectively. The data were collected at every 100ps and analysed [17].

Quantitative-Polymerase Chain Reaction (Qpcr)

qPCR was used to measure the amounts of mRNA in Human keratinocyte cell lines (HaCaT). DyNAmo Flash SYBR Green QPCRKit 500 Reaction was utilised to monitor the DNA amplification in real-time PCR method. Verso cDNA synthesis Kit was utilized for reverse transcription. HaCaT keratinocyte cell lines were treated with different concentrations (800, 1600, and 3200 M) of Chlorogenic acid and the total RNA was extracted at different time periods (1, 8, 24h) using Trizol method. The enzyme reverse transcriptase was used to convert the RNA template into complementary DNA by a procedure involving one cycle at 85 °C for 5 min, then 95 °C for 30sec for initial denaturation. Primer annealing was carried out at 72°C for 30 sec allowing the template to bind to both forward and reverse primers and a final extension for 5min repeated for 30cycle. Using real-time quantitative PCR, the amounts of TNF-α, IL-18 and MMP-9-mRNA in each sample were measured. The expression levels of TNF-α, IL-18 and MMP-9 mRNA transcript was normalized using β-actin mRNA. The sequence of reverse, forward primers of TNF-α, IL-18 and MMP-9 and reference genes are shown in Table 1. Fluorescence signals were detected at the elongation process of each PCR cycle. During the processes, a melting curve was created to examine the chance of primer-dimer production. The relative mRNA expression level of each gene was calculated by $2^{-\Delta\Delta Ct}$ method [18].

Table 1. Forward and Reverse Primer Sequence Used for Qpcr

Sr.No	Gene	Forward Primer Sequence	Reverse Primer Sequence
1	Tnf-A	Ccttcctgatcgtggcag	Gcttgagggtttgctacaac
2	Il-18	Cagtcagcaaggaattgtctc	Gaggaagcgatctggaagg
3	Mmp-9	Gccactactgtgcctttgagtc	Ccctcagagaatcgccagtact
4	B-Actin	Tggtggtaccaccatgtacc	Aggggccg Gactcatcgtact

Forward and reverse primer sequence of TNF-α, IL-18, MMP-9 and β-actin for qPCR studies (Ramalingam Shalini., et al 2023)

Preparation of Gel Base

The gel base was prepared by dissolving 1g of Carbopol-971 P in 50ml of distilled water with continuous agitation. Benzyl alcohol was added to Carbopol-971 P mixture. 2N NaOH was added to adjust the p^H to 6.8 to 7 and 1 and 2% of gel were prepared by adding Chlorogenic acid to carbopol gel under continuous agitation [19].

In Vivo Studies

Animals

Totally 26 Albino Wistar rats (250-350g) were selected for acute dermal toxicity and Circular Excision wound healing studies. Both the studies were carried out in the Department of Pharmacology, JSS College of Pharmacy, Ooty with due permission from the Institutional Animal Ethical Committee (Registration No: JSSCP/OT/IAEC/38/2019-20).

Acute Dermal Toxicity Study

Acute dermal toxicity study was carried out using OECD guide line 402. A total of 6 animals Were divided into 3 groups for the main study. 200mg/kg, 1000mg/kg and 2000mg/kg of gel was applied on the dorsal surface of group 1,2 and 3, respectively and observed for changes in the skin, fur, eyes and behavioural pattern for 14 days [20].

Circular Excision Wound Model

Excision wound models were created on animals that were divided into four groups of five animals in each group [21]. With group Ⅰ as control, group Ⅱ was treated as standard group (0.2% nitrofurazone) and group Ⅲ and Ⅳ were treated with 1% and 2% Chlorogenic acid, respectively. The open mask method using anaesthetic ether was utilized to anaesthetize all the animals [22]. A circular excisional wound model was created at the back of the rats with an area of 300 mm^2 and considered as a 0 day. The gel was applied every day till the 21st day. The wound area was measured and photographed on day 1, 7, 14 and 21 till a complete wound closure was observed. The progression of wound healing was measured [23] using the following formula,

Percentage Wound Closure= Initial wound size-specific day wound size/ Initial wound size*100

Histological Evaluation

The healed tissues were excised from the control, standard and treated animal group on day 21 and stained using haematoxylin and eosin to observe the histological changes takes place during wound healing

Statistical Analysis

The results of *in vitro* cell viability assay and the *in vivo* wound healing activity were expressed as mean±SEM. The results of scratch wound healing assay was expressed as percentage. The *in vivo* wound healing activity was analysed using two-way ANOVA variance followed by Turkey's multiple comparison test between the experimental groups using Graph pad prism version 9. qPCR results were analysed by by two-way ANOVA. P values less than 0.05 were considered as significant.

RESULTS

Extraction and Isolation

Chlorogenic acid was isolated from ethyl acetate fraction of methanolic extract with Rf value of 0.68. The yield of the compound was 30mg.

Spectral Studies

The compound (whitish powder) with molecular weight of 354.66 (m/z 355 $[M - H]^-$) indicates a molecular formula $C_{16}H_{18}O_9$. Its IR spectrum (NEAT, Beam splitter-KBr, Detector-DTGS KB) exhibits absorbance band at 3134.02 cm^{-1} indicating the presence of hydroxyl stretching followed by C=O stretching at 1635.67 and aromatic C=H stretching at 768.91 cm^{-1}. $_1$H-NMR (400MHz, DMSO) spectrum reveals single proton singlet at δ_H 9.1, 9.5, 3.3, 4.7, 5.03 indicating the presence of hydroxyl group at C_3, C_2, C_{16}, C_{13}, and C_{15} position, respectively. Single proton singlet at δ_H 12.3 indicates the presence of hydroxyl group in the carboxylic acid at C_{17} position and single proton doublet at δ_H 6.96 and 6.98 indicates the presence of CH group at C_7 and C_8 position, respectively. Two hydrogen doublet at δ_H 4.9 show the presence of CH_2 at C_{12} position. Single proton peak at δ_H 7.01, 6.7 doublet and 7.4 singlet signals indicates the presence of aromatic hydrogen at C_4, C_5 and C_1 position, respectively. Single hydrogen multiplet at δ_H 5.06 and 1.9 indicates the presence of CH group at C_{11} and C_{15}, respectively. Single hydrogen quartet at δ_H 1.7 reveals the presence of CH group at C_{16}. Two hydrogen triplets at δ_H 3.5 indicates the presence of CH_2 group at C_{14}. In the $_{13}$C-NMR (400MHz, DMSO) spectrum, signals at 36.22, 37.19, 68.04, 70.35, 70.88, 73.45, 115.73, 121.36, 125.58 and 148.34 reveals the presence of carbon at C_{12}, C_{14}, C_{11}, C_{13}, C_{15}, C_{16}, C_1, C_4, C_5 and C_6 respectively. Peaks at 165.72 and 174.94 indicate the presence of carbon in C=O and COOH, respectively. Signals at 114.27 and 114.76 indicate C-OH at C_2 and C_3, respectively and signals at 144.94 and 145.56 represent CH=CH at C_7 and C_8, respectively. The structure of the compound was further confirmed by LC-MS/MS analysis (Fig. 1). The compound was identified as Chlorogenic acid [24-25].

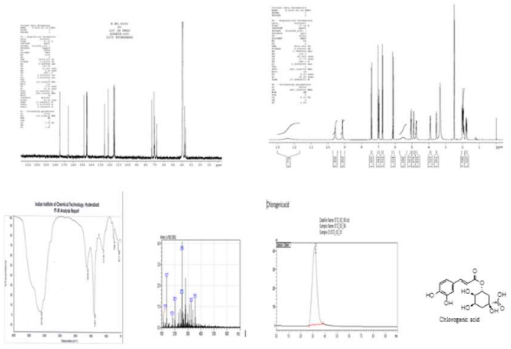

Fig. 1. $_{13}$C-NMR, $_{1}$H-NMR, FTIR, LC-MS/MS, HPLC and Structure of Chlorogenic Acid.

In Vitro Studies

In Vitro Fibroblast Cell Cytotoxicity Assay of the Isolated Compound by SRB

The percentage cell viability and migration of the human keratinocytes of the Chlorogenic acid was evaluated using HaCaT culture. The percentage cell viability of the compound against concentrations are shown in Table 2 and Fig. 2. The data reveal more than 85% cell viability at all the concentrations.

Table 2. Percentage of Cell Viability of Chlorogenic Acid in Hacat Cell Lines

Sr .No	Culture Conditions (µm)	Percentage Of Cell Viability
		Chlorogenic Acid
1	3200	74.09±2.51
2	1600	91.06±4.84
3	800	89.38±5.38
4	400	95.49±1.17
5	200	96.81±1.72
6	100	97.74±3.60
7	Cisplatin	24.53±0.00

mean±SEM, n=3, *****p <0.05*, ***p <0.05, *p <0.05*

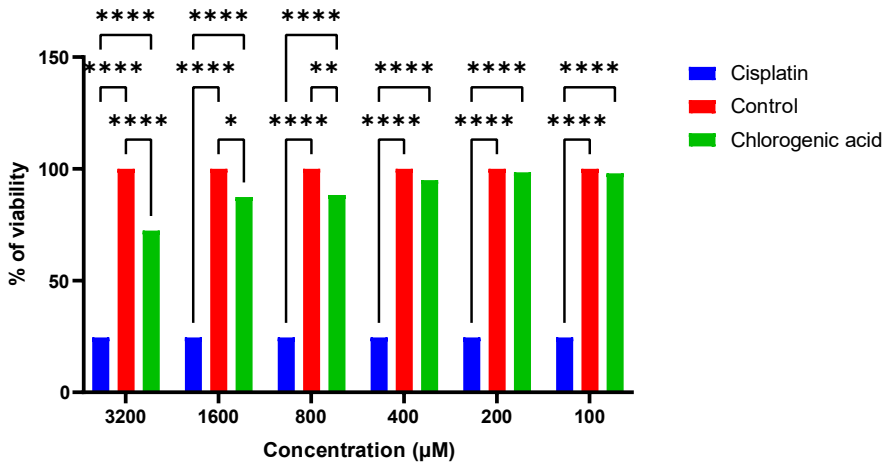

Fig. 2. % of Cell Viability of Chlorogenic Acid in Hacat Cell Lines

Effect of chlorogenic acid on the viability of human keratinocytes against different concentrations (100 to 3200µM). Each bar represents the percentage of cell viability against Cisplatin (100µM). Results are expressed as a mean±SEM, n=3, ****$p < 0.05$, **$p < 0.05$ vs Control.

Wound Scratch Test Assay

The percentage wound closure of the bioactive compound against various concentrations are shown in Table 3 and Fig. 3 and 4. The percentage of wound closure of the compound is higher at 18h. The compound shows 99 % wound closure at 24h.

Table 3. Percentage Of Wound Closure Of Chlorogenic Acid

S.No	Culture Conditions (µm)	% Wound Closure Chlorogenic Acid		
		12h	18h	24h
1	Control	17.5	25.4	34.2
2	Vc	15.33	27.52	36.1899.7
3	800	39.45	56.12	99.9
4	1600	44.3	62.9	99.7
5	3200	56.41	62.01	41.36
6	Itraconazole	21.8	33.65	

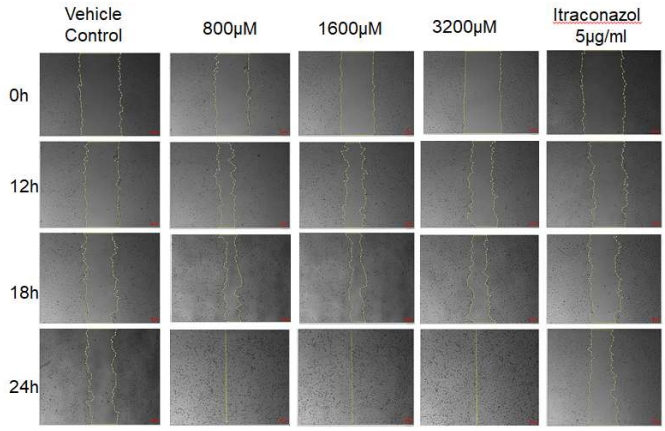

Fig. 3. *In Vitro* Migration Assay of Chlorogenic Acid

In vitro migration assay to calculate the % of wound closure of Chlorogenic acid. Different concentrations of Chlorogenic acid against wound area at 12, 18 and 24h. Cont- Control. VC-Vehicle control.

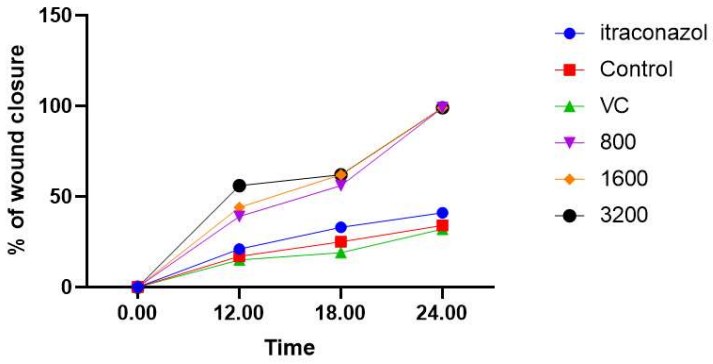

Fig. 4. Percentage of Wound Closure against Concentration of Chlorogenic Acid

In Silico Docking

The docking score of Chlorogenic acid with human wound healing targets, namely TNF-α, IL-12, IL-18, GM-CSF, MMP-2 and MMP-9 are shown in Table 4. The Docking score of Chlorogenic acid with MMP-9 is the lowest and found to be -9.4 kcal/mole. Chlorogenic acid forms 5 conventional hydrogen, 9 Van der Waals interaction, Pi-Alkyl bond and unfavourable acceptor-acceptor bond with MMP-9. The Glide score was determined using Schrodinger suit 2021-4 and shown in Table 5. The Glide score of Chlorogenic acid with MMP-9 is -8.677 kcal/mol.

Table 4. Docking Scores of Chlorogenic Acid with Various Wound Healing Targets

S.No	Target	Resolution	Docking Score (Kcal/Mol)
1	Tnf-A	$2.1a^0$	-7.3
2	Il-12	$2.01a^0$	-6
3	Il-18	$2.80a^0$	-8.1
4	Gm-Csf	$2.25a^0$	-6.8
5	Mmp-2		-7
6	Mmp-9	1.59 A^0	-9.4

The interaction between Chlorogenic acid with MMP-9 was visualized through BIOVIA Discovery studio visualizer tool and shown in Fig. 5a and b.

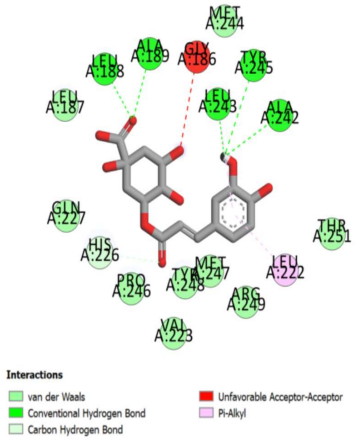

Fig.5a. 2D Interaction of Chlorogenic Acid with MMP-9

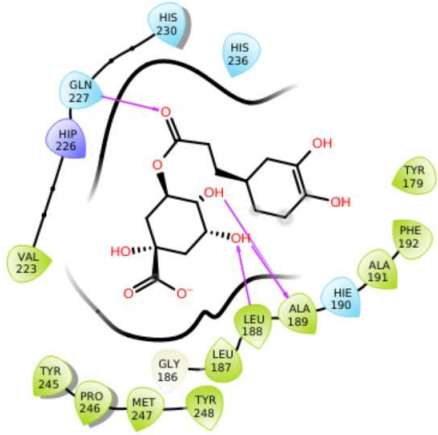

Fig. 5b. 2D Interaction of Chlorogenic Acid with MMP-9 Using Glide Module

Table 5. Glide Score of Chlorogenic Acid with MMP-9

Glide Gscore (Kcal/Mol)	Glide Evdw (Kcal/Mol)	Glide Ecoul (Kcal/Mol)	Glide Energy (Kcal/Mol)	Glide Emodel (Kcal/Mol)
-8.677	-29.854	-12.190	-42.044	-56.136

Pharmacokinetic, Physicochemical Properties and Toxicity Prediction Analysis

The pharmacokinetic and physicochemical properties of Chlorogenic acid were determined by SwissADME (http://www. swiss adme. ch/) server. The results of the pharmacokinetic, physicochemical properties and toxicity studies of Chlorogenic acid are shown in Table 6 and 7.

Table 6. Physicochemical Properties of Chlorogenic Acid

Mw	Rb	Tpsa	Xlogp3	Gi Absorption	Bbb Permeant	Cyp2d6 Inhibitor	Lipinski Violations	Pains Alerts	Synthetic Access
360.36	6	164.75	-1.88	Low	No	No	1	1	4.47

The computational TPSA of the compound is 164.75 Å2 showing its poor distribution. The volume of distribution and metabolism of a compound depends on CYP2D6 inhibitor; absence of the CYP2D6 inhibitor can increase the efficacy of a drug. The compound is thus non-mutagenic to Gram negative bacteria with medium risk to the hERG inhibition.

Table 7. Toxicity Study of Chlorogenic Acid

Algae Test	Ames Test	Carcino Mouse	Carcino Rat	Daphnia -At	Herg Inhibition	TA100-10RLI	TA100-NA	TA135-10RLI	TA1535 - NA
0.0415052	Mutagen	Positive	Negative	1.3461	Medium Risk	Negative	Negative	Negative	Positive

Mm/Gbsa

The binding free energy of the chlorogenic acid-MMP-9 complex was evaluated using MM/GBSA and the results are shown in Table 8. The contribution of van der Waals energy and non-polar solvation play an essential role in forming the strong and stable complex.

Table 8. Mm/Gbsa Binding Free Energy Calculation

Mm/Gbsa Δg Bind	Mm/Gbsa Δcoul	Mm/Gbsa Δh Bond	Mm/Gbsa Δlipo	Mm/Gbsa Δvdw
-46.4599	73.4417	-1.5453	-12.0937	-63.1273

MD Simulation

Molecular simulation was carried out to evaluate the structural and conformational modifications of Chlorogenic acid-MMP-9 complex. The RMSD graph was plotted for the ligand-protein complex for 100ns trajectory (Fig. 6). The RMSD of the protein Cα is observed in the range of 1.8-2.4 Å followed by a slight increase which stabilizes after 38ns and remain stable throughout the simulation except at 62-68ns and 98-100ns. The RMSF values of MMP-9 protein is stable near 70-85 and 120-140 residue index and present in α helix and β sheet, respectively (Fig. 7). GLN227 and Asp235 shows a high hydrogen bond interaction, shows strong binding (Fig. 9). The internal atom fluctuation of the ligand is shown in the Fig. 8. Other than hydrogen bond and water bridges, ionic and hydrophobic interactions also

play predominant role in binding (Fig. 9 & 10). The property of the ligand was characterised using ligand RMSD, radius of gyration, intramolecular hydrogen bonds, molecular surface area (MolSA), solvent accessible surface area (SASA) and polar surface area (PSA) (Fig. 11).

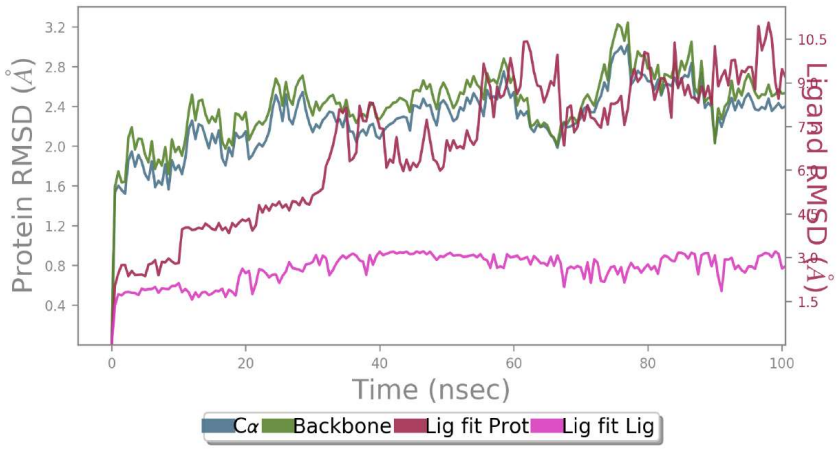

Fig. 6. RMSD of Chlorogenic Acid-MMP-9 Complex

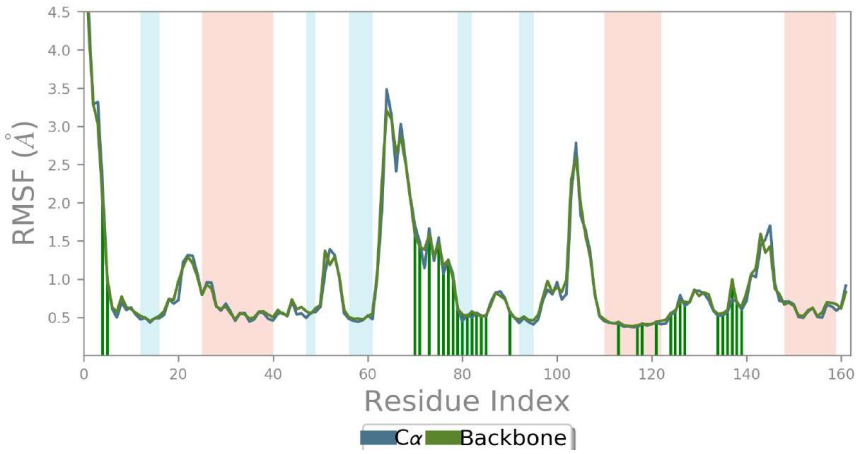

Fig. 7. RMSF of Chlorogenic Acid-MMP-9 Complex

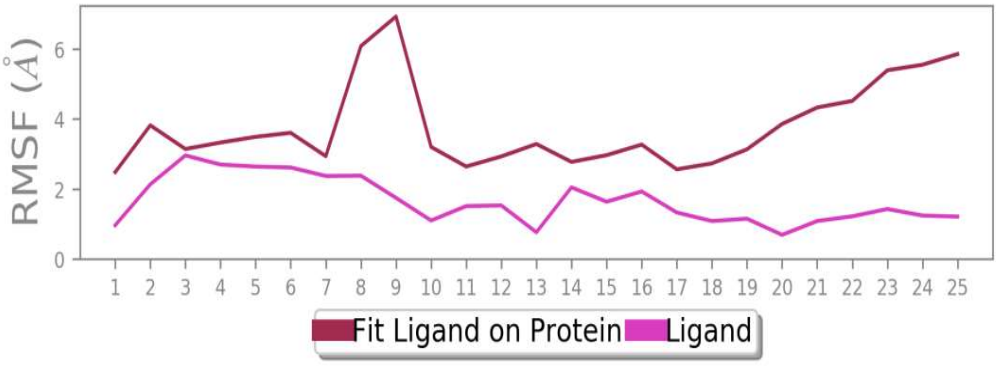

Fig. 8. Chlorogenic Acid Fluctuation With Respect To MMP-9

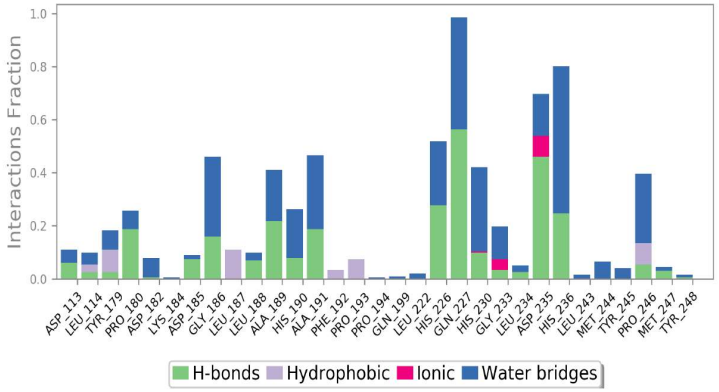

Fig. 9. Different Bonds Present in the Chlorogenic Acid-MMP-9 Complex

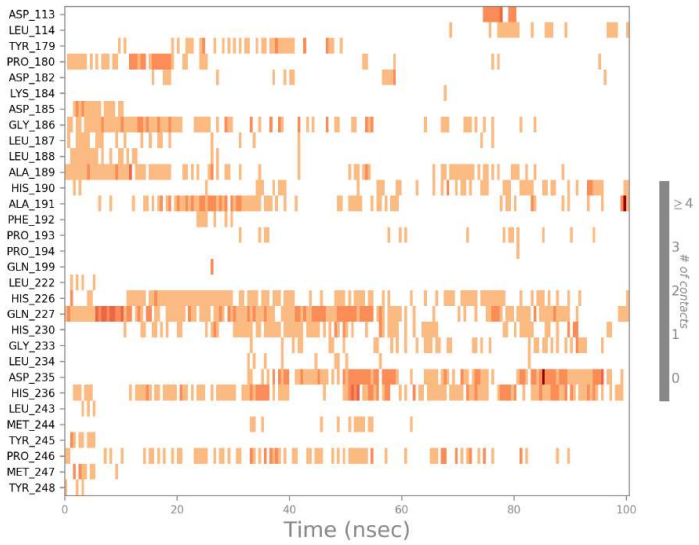

Fig. 10. Interaction Time of Each Amino Acid of the Protein with Ligand

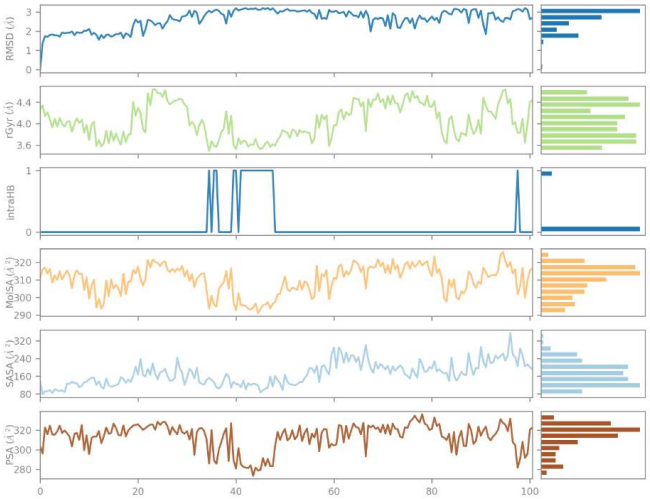

Fig. 11.Ligand Properties

Effect of Chlorogenic Acid on Mrna Expression of TNF-A, IL-18 and MMP-9

Proinflammatory cytokines, especially TNF-α, IL-18 and MMP-9 play considerable role in wound healing. The effect of Chlorogenic acid on TNF-α, IL-18 and MMP-9 in keratinocytes after the formation of scratch wound was investigated and the results are shown in **Fig. 12, 13 & 14**. The results also reveal that the compound upregulates TNF-α, IL-18 and MMP-9 mRNA expression in the early stages of wound repair.

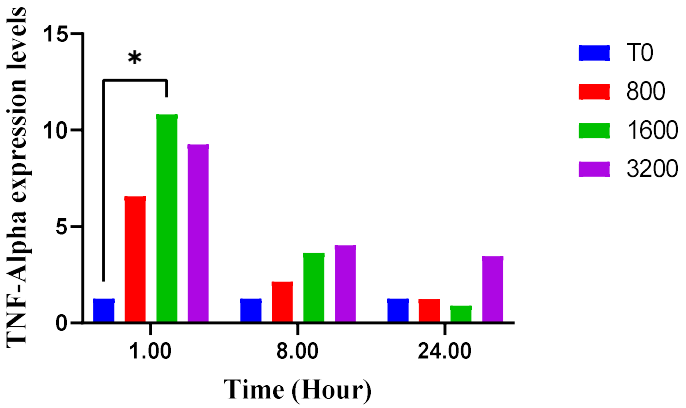

Fig. 12.Effect of Chlorogenic Acid on TNF-A Gene Expression

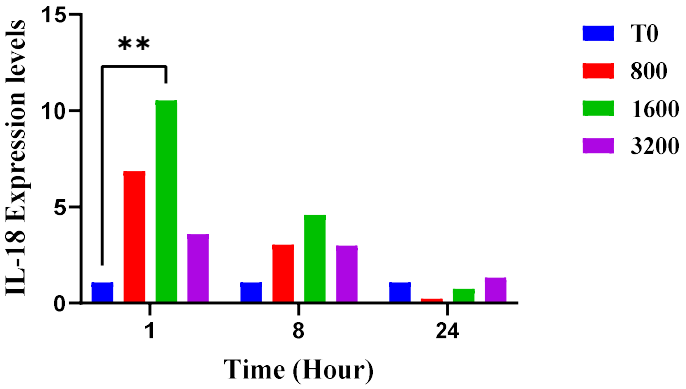

Fig. 13. Effect of Chlorogenic Acid on IL-18 Gene Expression

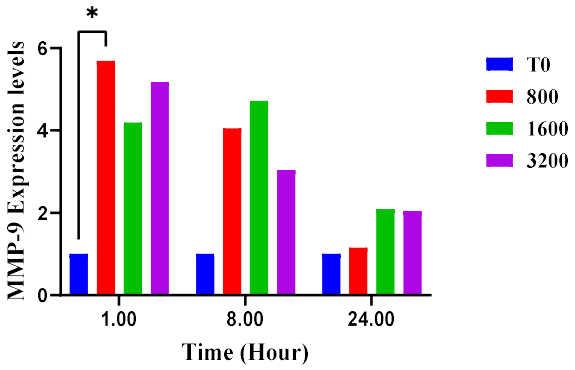

Fig. 14. Effect of Chlorogenic Acid on MMP-9 Gene Expression

In Vivo Studies

Acute Dermal Toxicity Study

The toxicity of Chlorogenic acid was evaluated using acute dermal toxicity study method. The compound with gel formulations are safe upto 2000mg/kg. The limit dose of 2000mg/kg does not show any toxicity and rats are active.

Circular Excision Wound Model

Chlorogenic acid with two different concentration of gel formulation were evaluated using circular excisional wound model. The percentage of wound contraction against days is shown in Table 9 and Fig. 15 & 16. Chlorogenic acid with 1 and 2% shown dose dependent activity but 2% did not show any significance compared to control. Histological studies show significant collagen content, inflammatory cells and angiogenesis (Fig. 17).

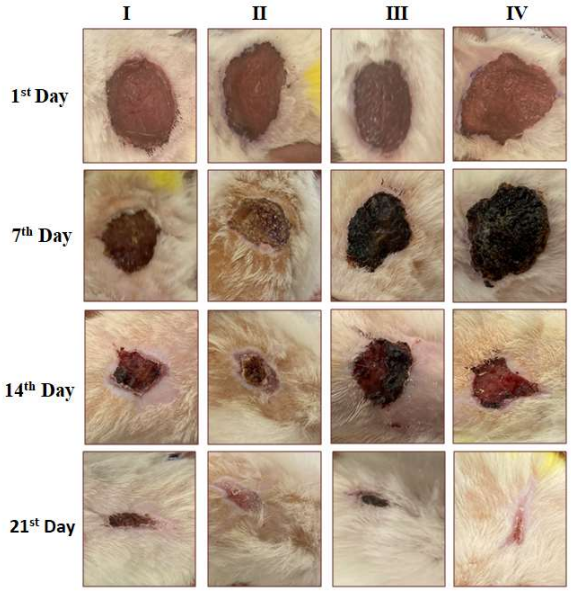

Fig. 15. Excision Wound Healing Model

(Ramalingam Shalini., et al 2023) Circular excisional wound healing on day 1, 7, 14 and 21st day, Ⅰ-Control, Ⅱ- Nitrofurazone, Ⅲ-1% Chlorogenic acid, Ⅳ-2% Chlorogenic acid.

Table 9. The Percentage of Wound Closure

Day	% Of Wound Closure			
	Control	Nitrofurazone	1% Chlorogenic Acid	2% Chlorogenic Acid
1	5.76±0.76	11.74±1.51	6.06±1.45	10.52±1.86
7	26.12±1.89	34.37±5.52	34.66±2.71	29.43±9.55
14	66.55±2.43	78.62±1.89	69.10±1.68	72.21±4.61
21	83.46±0.84	96.15±0.98	86.55±2.17	91.28±2.24
28	91.03±0.89	99.75±0.19	91.25±1.76	94.18±0.96

mean ±SEM*p <0.05, **p <0.05 vs Control.

In vivo excisional wound model was utilized to calculate the % of wound closure of Chlorogenic acid. The 1 and 2% of Chlorogenic acid was treated to calculate the wound area at 7, 14, 21 and 28 days. n=5 animals in each group, Control-without treatment, Standard drug-nitrofurazone.

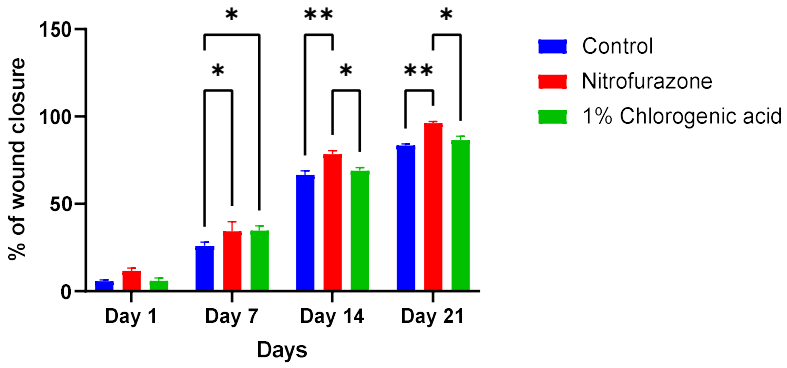

Fig. 16. Percentage of Wound Closure

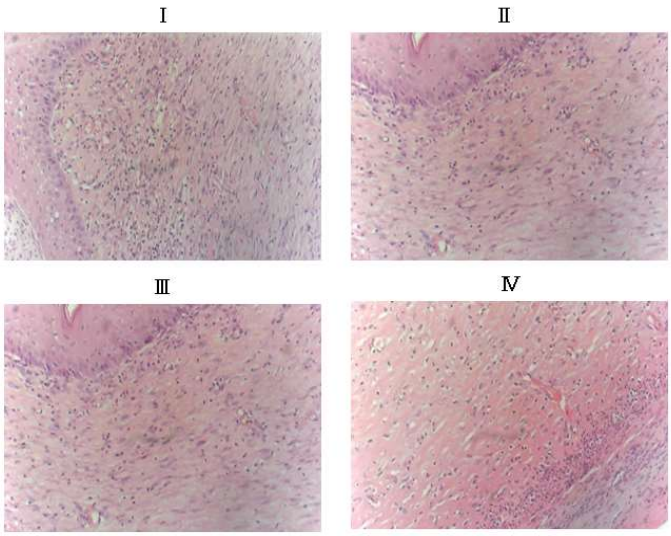

Fig. 17. Histological Studies

Ⅰ-Control group, Ⅱ-Standard, Ⅲ-1% Chlorogenic acid, Ⅳ-2% Chlorogenic acid

DISCUSSION

The leaf paste of plant, *Eupatorium glandulosum* H. B & K, has been traditionally used to treat wounds by the Badagar, Irular and Thoda communities of the Nilgiri district, India [26]. In the present study the traditional claims were validated using modern scientific methods.

Chlorogenic acid was isolated from the ethyl acetate fraction and shows a higher migration percentage in HaCaT cell lines. The compound enhances the migration of NHEKs cells and shows the highest level of wound closure at an early period of time. This compound has been earlier reported to delay the migration of fibroblast (NHDF) cell line [27].

Further the relationship between the wound healing activity and the structure of the compound was evaluated using *in silico* docking studies. The compound shows significant binding energy with the wound healing targets, TNF-α, IL-18 and MMP-9. The binding energy of Chlorogenic acid with MMP-9 is the highest. Based on this, the stability of the Chlorogenic acid-MMP-9 complex was evaluated using simulation studies. GLN227 and Asp235 amino acids were found to be responsible for the strong binding of the Chlorogenic acid to MMP-9. The results reveal that the complex is stable throughout the study with minor fluctuations.

The major role of TNF- α is to recruit various inflammatory cells such as neutrophils and macrophages and help in the formation of extracellular matrix by modulating fibroblasts, vascular endothelial cells and keratinocytes [28-29].

Chlorogenic acid upregulates IL-18 during early stages of healing and play a predominant role in recruiting polymorphonuclear neutrophils, neutrophil extracellular trapping (NET) and stimulate the production of IFN-γ and prevent the formation of fibrosis [30-31]. Chlorogenic acid does not prolong the expression of IL-18. The compound, however, increases MMP-9 during early and mid-period of healing which indicates its role in recruiting inflammatory cells, proliferation, migration of keratinocytes and angiogenesis [14]. The wound healing activity of Chlorogenic acid was evaluated using excisional wound model. Carbopol-971 gel with 1% Chlorogenic acid shows significant wound closure.

CONCLUSION:

The plant, *Eupatorium glandulosum,* is one of the traditional wound healing plants in Nilgiris. The bioactive compound, Chlorogenic acid, was isolated from the ethyl acetate fraction of fresh plant methanolic acid. The *in silico* molecular docking studies against various wound healing targets show significant binding energy with the wound healing targets, TNF-α, IL-18 and MMP-9. Molecular dynamic study shows that Chlorogenic acid-MMP-9 complex is very stable. qPCR analysis of TNF-α, IL-18 and MMP-9 mRNA expression reveal its role in the early stages of wound healing. Chlorogenic acid also shows significant wound closure in circular excisional wound healing model. Chlorogenic acid is, therefore, a possible drug/lead for wound healing.

Acknowledgement:

Authors would like to thank JSS college of Pharmacy and JSS School of Life Science, Ooty for the facilities offered. In addition, the authors would like to thank JSS Medical College, Mysuru for providing *in vitro* cell lines.

Funding:

This research work was not funded by any agencies.

Conflict of Interest

The authors declare no conflict of interest regarding the contents of the present manuscript.

REFERENCE

1. [1] Hu,X., Qina, N., Xue, J., Li, S., Huang, X., Sun, J., Xu, F., Li, Z., Li, D and Hua, H. (2019) Dehydrodiconiferyl alcohol from Silybum marianum (L.) Gaertn accelerates wound healing via inactivating NF-KB pathways in macrophages. Royal Pharmaceutical Society, Journal of Pharmacy and Pharmacology, ** (2019), pp. **–**
2. [2] Şahin, F., Koçak, P., Güne, M,Y., Özkan, I., Yıldırım1, E & Kala, E,Y. (2018) In Vitro Wound Healing Activity of Wheat-Derived Nanovesicles. Applied Biochemistry and Biotechnology.
3. [3] Yang X, Kui L, Tang M, Li D, Wei K, Chen W, Miao J and Dong Y. (2020) High-Throughput Transcriptome Profiling in Drug and Biomarker Discovery. Front. Genet. 11:19.doi: 10.3389/fgene.2020.00019
4. [4] Suntar, I,P., Akkol, E,K., Yalçin, F,N., Koca, U., Keles H., Yesilada, E. (2010). Wound healing potential of *Sambucus ebulus* L. leaves and isolation of an active component, quercetin 3-O-glucoside. J Ethnopharmacol. 129(1): 106-14.
5. [5] Annan K and Houghton, P, J. (2010). Two novel lupane triterpenoids from *Paullinia pinnata* L. with fibroblast stimulatory activity. Journal of Pharmacy and Pharmacology, 62: 663–668
6. [6] Ghosh, S., Samanta, A., Mandal, N.B., Bannerjee, S., Chattopadhyay, D. (2012). Evaluation of the wound healing activity of methanol extract of *Pedilanthus tithymaloides* (L.) Poit leaf and its isolated active constituents in topical formulation. J Ethnopharmacol. 142(3):714-22.
7. [7] Yadav, E., Singh, D., Yadav, P., & Verma, A. (2017). Attenuation of dermal wounds via downregulating oxidative stress and inflammatory markers by protocatechuic acid rich n -butanol fraction of *Trianthema portulacastrum Linn*. in wistar albino rats. Biomedicine & Pharmacotherapy, 96, 86–97. doi:10.1016/j.biopha.2017.09.125
8. [8] Turabelidze A., & Dipietro, LA. (2011), Inflammation and wound healing. Endodontic Topics, *24(1), 26–38.* doi:10.1111/etp.12012
9. [9] Silpa, M., Suresh, J., Babu, S., Hamsalakshmi, A., (2018). Review on *Eupatorium glandulosum*. International Journal of Pharmacognosy and Phytochemical Research 10(4),157-159
10. [10] Ramalingam, S., Chandrasekar, M.J.N., Nanjan, M.J., (2022). Plant-based Natural Products for Wound Healing: A Critical

Review. Current Drug Research Reviews, 14(1), 37-60.

11. [11] Balekar, N., Katkam, N.G., Nakpheng, T., Jehtae, K., Srichana, T., (2012). Evaluation of the wound healing potential of *Wedelia trilobata* (L.) leaves. Journal of Ethnopharmacology. 141,817– 824. doi: 10.1016/j.jep.2012.03.019.
12. [12] Jose A, Chaitanya MVNL, Kannan, E and Madhunapantula S,V. (2018) Tricaproin Isolated From *Simarouba glauca* Inhibits the Growth of Human Colorectal Carcinoma Cell Lines by Targeting Class-1 Histone Deacetylases. Front. Pharmacol. 9:127.
13. [13] Buia, N,T., Hoa, M,T., Kima, Y,M., Limb, Y., (2014). Cho M. Flavonoids promoting HaCaT migration: II. Molecular mechanism of 4,6,7-trimethoxyisoflavone via NOX2 activation. Phytomedicine 21;570–577
14. [14] Ramalingam Shalini, Moola Joghee Nanjan Chandrasekar, Moola Joghee Nanjan, SubbaRao V Madhunapantula, Medha Karnik, Jubie Selvaraj, Gonna Nandhi Krishnan Ganesh., 1- Tetracosanol isolated from the leaves of *Eupatorium glandulosum*, accelerates wound healing by expressing inflammatory cytokines and matrix metalloproteinase. Journal of Ethnopharmacology. 2023;315:116654. Doi: 10.1016/j.jep.2023.116654.
15. [15] Dallakyan, S., & Olson, A. J. (2014). Small-Molecule Library Screening by Docking with PyRx. Chemical Biology, 243–250.
16. [16] Kalirajan Rajagopal, Potlapati Varakumar, Baliwada Aparna, Gowramma Byran and Srikanth Jupudi. (2021). Identification of some novel oxazine substituted 9-anilinoacridines as SARS-CoV-2 inhibitors for COVID-19 by molecular docking, free energy calculation and molecular dynamics studies. Journal of Biomolecular Structure And Dynamics. 39 (15): 5551–5562
17. [17] Srikanth Jupudi., Kalirajan Rajagopal., Sankaranarayanan Murugesan., Banoth Karan Kumar., Kannan Raman, Gowramma Byran., Jayakuamar Chennaiah., Velayutham pillai Muthiah., Bharathi Dasan P., Sathianarayanan Sankaran. (2022). Identification of Papain-Like Protease inhibitors of SARS CoV-2 through HTVS, Molecular docking, MMGBSA and Molecular dynamics approach. South African Journal of Botany 151:8291
18. [18] Li, Hua-Liang., Liu, Xiao-Tian., Huang, Shao-Min., Xiong, You-Xiong., Zhang, Zi-Ran., Zheng, Ya-Hui., Chen, Qing-Xi., Chen, Qiong-Hua. (2021). Repair function of essential oil from *Crocodylus Siamensis (Schneider, 1801)* on the burn wound healing via up-regulated growth factor expression and anti-inflammatory effect. Journal of Ethnopharmacology 264; 113286
19. [19] Meghana, G., Narayana Reddy Karri, V.V.S., Talluri, S.V., Raviteja, G., Chennareddy, S.R., and Ganesh, G.N.K.. (2014). Formulation and evaluation of Tolnaftate loaded topical liposomal gel for effective skin drug delivery to treat fungal diseases. J. Chem. Pharm. Res. 6(10):856-866
20. [20] Mekonnen, A., Sidamo, T., Asres, K., Engidawork, E. (2013). In vivo wound healing activity and phytochemical screening of the crude extract and various fractions of *Kalanchoe petitiana* A.Rich (Crassulaceae) leaves in mice. Journal of Ethnopharmacology 145:638–646
21. [21] Dev, S.K., Choudhury P.K, Rajnish Srivastava, Maya Sharma. (2019). Antimicrobial, anti-inflammatory and wound healing activity of polyherbal Formulation. Biomedicine & Pharmacotherapy 111; 555–567
22. [22] Shivhare, Y., Singour, P.K., Patil, U.K., Pawar, R.S. (2010). Wound healing potential of methanolic extract of *Trichosanthes dioica* Roxb (fruits) in rats. Journal of Ethnopharmacology 127: 614–619
23. [23] Silambujanaki, P., Chandraa, C,B, T., Anil Kumar, K., Chitra, V. (2011) Wound healing activity of *Glycosmis arborea* leaf extract in rats. Journal of Ethnopharmacology 134; 198–201
24. [24] Suarez-Quiroz, M.L., Alonso Campos, A., Valerio Alfaro, G., González-Ríos, O., Villeneuve, P., Figueroa-Espinoza, M.C. (2014). Isolation of green coffee chlorogenic acids using activated carbon. J. Food

Compos. Anal. 33(1), 55–58. DOI:10.1016/j.jfca.2013.10.005

25. [25] Park, J.B. (2013). Isolation and quantification of major chlorogenic acids in three major instant coffee brands and their potential effects on H2O2-induced mitochondrial membrane depolarization and apoptosis in PC-12 cells. Food Funct, 4(11), 1632. doi: 10.1039/c3fo60138b.
26. [26] Sasikumar, J.M., Pichai Anthoni Doss, A., Doss, A., (2005). Antibacterial activity of *Eupatorium glandulosum* leaves. Fitoterapia 76, 240 – 243. doi.org/10.1016/j.fitote.2004.12.001
27. [27]Sara E. Moghadam, Samad N. Ebrahimi, Peyman Salehi, Mahdi Moridi Farimani, Matthias Hamburger, and Ehsan Jabbarzadeh (2017). Wound Healing Potential of Chlorogenic Acid and Myricetin-3-O-β-Rhamnoside Isolated from Parrotia persica. Molecules. ; 22(9): doi:10.3390/molecules22091501
28. [28] Ritsu, M. et al., (2016). Critical role of tumor necrosis factor-α in the early process of wound healing in skin, Journal of Dermatology & Dermatologic Surgery,http://dx.doi.org/10.1016/j.jdds.2016.09.001
29. [29] Tomohiro Banno S, Alix Gazel, and Miroslav Blumenberg., (2004). Effects of Tumor Necrosis Factor-α (TNF-α) in Epidermal Keratinocytes Revealed Using Global Transcriptional Profiling. The Journal of biological Chemistry. 279 (31): 32633–32642
30. [30] Kampfer, H., Kalina, U., Muhl, H., Pfeilschifter, J., and Frank, S. (1999). Counterregulation of Interleukin-18 mRNA and Protein Expression during Cutaneous Wound Repair in Mice. *J.Invest Dermatol* 113:369–374
31. [31] Artlett C.M. (2013). Inflammasomes in wound healing and fibrosis. *J Pathol*;.229: 157–167